

## Solutions of Negatively Charged Graphene Sheets and Ribbons

Cristina Vallés,<sup>†</sup> Carlos Drummond,<sup>†</sup> Hassan Saadaoui,<sup>†</sup> Clascidia A. Furtado,<sup>‡</sup> Maoshuai He,<sup>†</sup>  
Olivier Roubeau,<sup>†</sup> Luca Ortolani,<sup>§,||</sup> Marc Monthieux,<sup>§</sup> and Alain Pénicaud<sup>\*,†</sup>

Centre de Recherche Paul Pascal - CNRS, Université de Bordeaux, Av. Schweitzer, 33600 Pessac, France, Centro de Desenvolvimento da Tecnologia Nuclear-CDTN/CNEN, 31270-901, Belo Horizonte-MG, Brazil, Centre d'Elaboration des Matériaux et d'Etudes Structurales (CEMES), UPR-8011 CNRS, BP 94347, 31055 Toulouse cedex 4, France, and University of Bologna and CNR IMM-Bologna, Via Gobetti 101, 40129 Bologna, Italy

Received February 22, 2008; Revised Manuscript Received October 19, 2008; E-mail: penicaud@crpp-bordeaux.cnrs.fr

Graphene, an infinite, one atom thick, 2-D array of carbon hexagons is considered the reference for all  $sp^2$ -derived allotropic forms of carbon (graphite, fullerenes, nanotubes, schwarzite). Previously considered a virtual object, its recent experimental availability has stirred an ever-increasing activity<sup>1</sup> since the first samples were produced in 2004.<sup>2</sup> Far reaching applications such as patterned single-electron transistors,<sup>1</sup> ultimate gas sensors able to detect one molecule,<sup>3</sup> as well as high volume applications such as mechanically reinforced composites<sup>4</sup> are envisioned. In their original work, Geim et al. used graphene flakes obtained by micromechanical cleavage of graphite.<sup>2</sup> Since then, graphene deposits have also been produced by SiC epitaxy.<sup>5</sup> Both techniques are limited in terms of quantities of available samples. To overcome these limitations, in the past few months, there has been a large number of attempts to produce graphene flakes by a liquid phase route. These include reduction of water soluble graphite oxide,<sup>6–10</sup> sonication assisted dispersion in dimethylformamide<sup>11</sup> or *N*-methylpyrrolidone (NMP),<sup>12</sup> sonication assisted dispersion with PmPV in dichloroethane,<sup>13</sup> and sonication-aided dispersion of oleum-intercalated graphite.<sup>14</sup> All of these routes have successfully provided graphene flakes deposited on substrates, albeit with varied advantages or drawbacks, the main drawback being the probable existence of defects, coming from incomplete graphite oxide reduction or shortened flakes when using sonication.<sup>15</sup> Additionally, a few attempts have been made at dissolving graphite by functionalization of either graphite itself<sup>16</sup> or acid-oxidized graphite.<sup>17,18</sup> Given the interest in graphene physics, it is highly desirable to have varied dissolution/dispersion routes in order to increase samples availability. We present here a mild dissolution route, starting from neutral graphite and avoiding any kind of sonication that yields large size graphene flakes. Following a previous work on mild dissolution of carbon nanotubes,<sup>19</sup> we show here that alkali metal graphite intercalation compounds (GICs)<sup>20</sup> readily and spontaneously exfoliate in *N*-methylpyrrolidone (NMP), yielding stable solutions of negatively charged graphene sheets and ribbons.<sup>21</sup> These sheets can be deposited on a variety of substrates, thus enabling a large scale route to graphene deposits and composites.

The sonication-free, mild dissolution of graphite only requires the addition of electrons (reduction) to the graphene layers. This is done by synthesizing well-documented GICs, such as the ternary potassium salt  $K(\text{THF})_x\text{C}_{24}$  (THF = tetrahydrofuran,  $x = 1–3$ ).<sup>22</sup> Exposure of this potassium GIC to NMP readily and spontaneously exfoliates the intercalated graphite and yields air-sensitive solutions of reduced graphene sheets, affording a virtually unlimited amount

of one-atom thick layers. The graphene sheets can be deposited from these solutions onto a variety of substrates, and have been characterized by atomic force microscopy (AFM), ambient scanning tunneling microscopy (STM), multiple beam interferometry (MBI), optical microscopy, X-ray photoelectron spectroscopy (XPS), high resolution transmission electron microscopy (HRTEM), and Raman spectroscopy, all evidencing deposition of graphene or few-layers sheets. Once dried, the deposits can be freely air-exposed and the graphene layers are oxidized back to the neutral state.<sup>23</sup> These solutions have been reproducibly obtained with all kinds of graphite tested so far (i.e., small grain graphite obtained by filing down a graphite electrode,<sup>24</sup> natural and expanded graphite, and highly oriented pyrolytic graphite (HOPG)).

Polyelectrolyte systems can often be dissolved even in unfavorable solvents due to the entropy gain associated with dissolving the counterions.<sup>25</sup> Carbon nanotubes (CNT) are macromolecules, and solutions of CNTs were obtained quite recently simply by dissolving a salt of carbon nanotubes in polar solvents.<sup>19</sup> By analogy with solutions of nanotube salts, we reasoned that graphite intercalation compounds (GIC) may be soluble at least partially in polar solvents. A potassium GIC was thus prepared in controlled inert atmosphere according to literature procedures<sup>26</sup> and was found to be soluble in *N*-methylpyrrolidone, affording colored, aggregates-free solutions, after mild centrifugation to remove the insoluble material. A control experiment with neutral graphite gave a colorless transparent liquid after the same procedure. Dry extract of the solution gives a 20% yield for the dissolution procedure and a concentration of 0.15 mg/ml of dissolved material. Potassium analysis (by atomic absorption spectroscopy) yields a potassium content of 36 ppm ( $\pm 10\%$ ) that translates in between 0.1 and 0.5 mg/ml dissolved material, depending on the molecular formula considered, consistently with the dry extract measurement. If air-exposed, the solutions turn colorless in ca. 2 days. Optical microscopy of the solutions showed no aggregates, whereas the oxidized solutions revealed ca. 20  $\mu\text{m}$ -size aggregates (Supporting Information, Figure S1).

Deposits were performed on different substrates. After deposition, removal of solvent and rinsing, the supports were handled in air. XPS analysis (Supporting Information) on either  $\text{SiO}_2$  or HOPG show no detectable nitrogen signal, implying that all NMP has been removed by the rinsing procedure. No potassium could be detected: by analogy with  $\text{C}_{60}$ <sup>27</sup> and nanotubes,<sup>23</sup> potassium ions are expected to form oxide or hydroxide upon ambient air exposure, which was removed by the rinsing procedure.

Ambient STM images have been obtained by drop casting the solution on HOPG substrates. Figure 1 shows a graphene flake laying on a HOPG step. The measured height difference between the substrate and the top of the flake is 0.36 nm, that is, that of a

<sup>†</sup> Université de Bordeaux.<sup>‡</sup> Centro de Desenvolvimento da Tecnologia Nuclear-CDTN/CNEN.<sup>§</sup> Centre d'Elaboration des Matériaux et d'Etudes Structurales (CEMES).<sup>||</sup> University of Bologna and CNR IMM-Bologna.

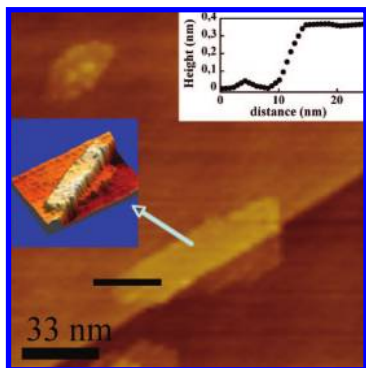


**Figure 1.** Ambient STM image of a filed-down graphite deposit drop casted from solution on a HOPG substrate, showing a graphene flake, laying on a HOPG step. Height scan inset shows a height difference of 0.36 nm between substrate and flake. Similar results have been obtained on a vast number of flakes (see Supporting Information).

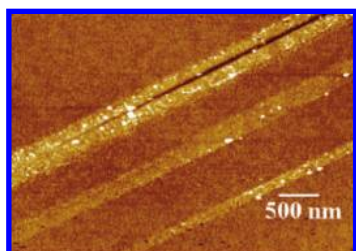


**Figure 2.** Tapping mode AFM image of a deposit performed by dip-coating of a graphene solution (from expanded graphite) onto Si/SiO<sub>2</sub> wafer. Height measurements give between 0.8 and 1.3 nm for the three ribbons (other images in Supporting Information).

single graphene layer. For AFM, deposits on Si/SiO<sub>2</sub> wafers (Figure 2) and nickel-modified muscovite mica (Figure 3) were obtained by dip coating in the solutions. Figure 2 shows three parallel ribbons, having a height of ca. 1.2 nm. This height has repeatedly been reported in the literature for one-atom thick graphene on Si/SiO<sub>2</sub> wafers.<sup>28</sup> Figure 3 (on mica) shows the end of a similar graphene ribbon; the whole object could be followed and is ca. 40  $\mu$ m long (Supporting Information). Note that the height measured for this ribbon laying over mica is ca. 0.4 nm, that is, of the order of the actual graphene thickness, contrary to Si/SiO<sub>2</sub> wafers where a single layer translates into ca. 1 nm height.<sup>28</sup>

The same dip-coating treatment with two silver layers evaporated on each side of the mica/graphene stack allows precise height measurements of the deposits on a large scale through multiple beam interferometry (Supporting Information). A typical height profile and a photograph of the coated mica surface are presented in Figure 4. Such measurements revealed stripes several tens by several hundreds micrometers of ca. 0.34 nm thickness. Given the poor lateral resolution, these could also be a collection of contiguous narrow ribbons in agreement with the AFM images. Additionally, the flakes deposited on a modified Si/SiO<sub>2</sub> wafer (Surf, Sarfus Technology) have been imaged by differential interference contrast (DIC) optical microscopy in a manner similar to the procedure on Si/SiO<sub>2</sub> substrates.<sup>29</sup> By comparison with standards of known heights, heights of 0.3 and 0.7 nm were obtained for deposited ribbons (Figure S6–1, Supporting Information).

Raman measurements were performed on starting materials, solutions, and deposits, evidencing the graphitic nature of all sheets and ribbons. The spectra are shown in the Supporting Information. For both solutions in NMP and deposits, the G band is clearly present, upshifted, as expected for a single-layer doped graphene.<sup>30</sup>

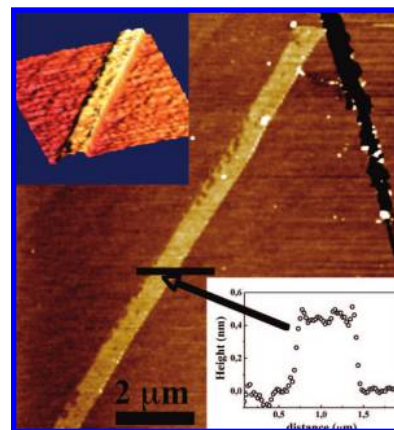


**Figure 3.** Tapping mode AFM image of a deposit performed by dip-coating of a graphene solution (from expanded graphite) onto mica. Height measurements of the ribbon shows a height of 0.4 nm; the full length of the ribbon is ca. 40  $\mu$ m (Supporting Information).

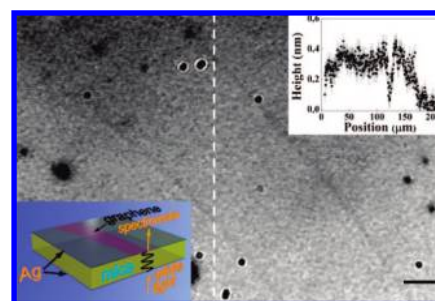


**Figure 4.** Optical microscopy image of a HOPG deposit on mica, sandwiched between two 45 nm thick silver mirrors. The scale bar (bottom right corner) is 25  $\mu$ m long. The top inset shows the height profile measured along the dotted line on the image. The left inset is a schematic view of the silver–mica–graphene–silver stack.

Additionally, a symmetrical (as expected for graphene) G' band is seen in the 2500–2900  $\text{cm}^{-1}$  region, downshifted from the starting graphite position. It has recently been shown that doping can severely affect Raman spectra of graphene flakes.<sup>31,32</sup> A detailed analysis of Raman spectra of our deposits with varying reoxidation procedure is underway.

Finally, HRTEM has been performed. Figure 5 shows a multi-graphene flake (see caption).

Preliminary conductivity measurements have been performed on interdigitated electrodes dip-coated into the solution. The room temperature *I*–*V* curves were linear with a resistance of 235 and 370 ohms for two different devices (Supporting Information). This demonstrates the conducting nature of the deposits.

GICs, which have been known and extensively studied for at least 40 years, are composed of positively—or negatively—charged graphite layers with counterions intercalated between each layer for stage 1 GICs.<sup>20</sup> Previous works on Li<sub>2</sub>Mo<sub>6</sub>Se<sub>6</sub><sup>33</sup> and alkali salts of single-walled nanotubes<sup>34</sup> have shown that one-dimensional, rigid, charged macromolecules (i.e., polyelectrolytes) could be dissolved in polar aprotic solvents.<sup>19,35</sup> The solutions described in this report show indeed similar physics for the dissolution of extended, two-dimensional objects, that is, entropy driven solvation of the cations, yielding a true thermodynamic solution. Deposits from these solutions afford large size graphene flakes and ribbons. It is remarkable that the graphene ribbon imaged over a mica surface (Figure 3) gives a height value (0.4 nm) close to the actual graphene height (0.35 nm).

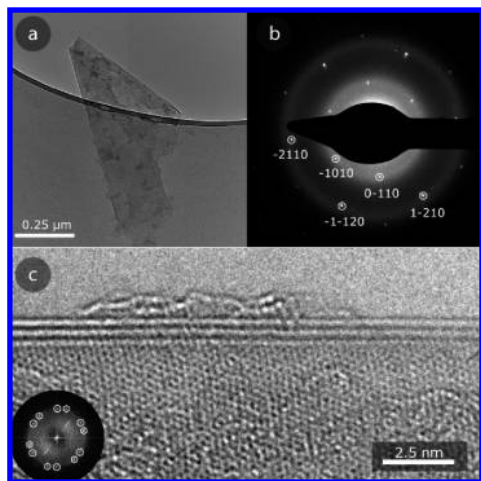


**Figure 5.** (a) TEM image of a multigraphene flake partially folded over itself. (b) Electron diffraction image from the tip unfolded region with some indexed graphene reflections. Analysis of the diffraction peaks intensity (Supporting Information) confirms a multilayer nature and ABAB stacking. (c) Cs-corrected HRTEM image, obtained at 80 kV to avoid electron damage using a Tecnai F20 (SACTEM-Toulouse), showing 002 fringes, and lattice fringes curvature, due to folding of the flake. Analysis of the number of fringes unambiguously determines the number of layers as 3.

The reversible addition of electrons to graphite presented here provides a simple and clean route to exfoliate and dissolve large graphene flakes and ribbons. Through controlled deposition and subsequent patterning, graphene-based electronic circuits can be envisioned. Furthermore, since the graphene flakes are homogeneously dissolved, graphene-based composites may be prepared by mixing graphene and polymers or by in situ polymerization within the graphene solutions.

**Acknowledgment.** We thank C. Hérold for a gift of expanded graphite, A. Mansour for a gift of filed-down graphite powder, N.G. Rosa (Nacional de Grafite) for graphite samples, P. Croguennoc (Nanolane) for Surf wafers and Figure S6-I, B. Raquet and W. Escoffier for help with the conductivity measurements, F. Guillaume, J.-L. Bruneel, J. B. Salmon and B. Pavageau for help with Raman measurements, P. Delhaès, J. E. Fischer and P. Poulin for critical reading of the manuscript, and A. Ferrari for continuous and encouraging support. We acknowledge support from CNRS, the ANR (Tricotra), and GDR-I 2756. C.A.F. acknowledges CNEN, CNPq, FAPEMIG, and MCT/Brazilian Carbon Nanotube Network for financial support.

**Supporting Information Available:** Preparation of the GICs and their solutions, preparation and imaging of the deposits, details of the interferometry and DIC measurements, additional STM and AFM images, XPS detailed analysis, Raman spectra and discussion, HRTEM details, complete ref 12, conductivity measurements. This material is available free of charge via the Internet at <http://pubs.acs.org>.

## References

- (1) Geim, A. K.; Novoselov, K. S. *Nat. Mater.* **2007**, *6*, 183–191.
- (2) Novoselov, K. S.; Geim, A. K.; Morozov, S. V.; Jiang, D.; Zhang, Y.; Dubonos, S. V.; Grigorieva, I. V.; Firsov, A. A. *Science* **2004**, *306*, 666–669.
- (3) Schedin, F.; Geim, A. K.; Morozov, S. V.; Hill, E. W.; Blake, P.; Katsnelson, M. I.; Novoselov, K. S. *Nat. Mater.* **2007**, *6*, 652–655.
- (4) Stankovich, S.; Dikin, D. A.; Dommett, G. H. B.; Kohlhaas, K. M.; Zimney, E. J.; Stach, E. A.; Piner, R. D.; Nguyen, S. T.; Ruoff, R. S. *Nature* **2006**, *442*, 282–286.
- (5) Berger, C.; Song, Z.; Li, X.; Wu, X.; Brown, N.; Naud, C.; Mayou, D.; Li, T.; Hass, J.; Marchenkov, A. N.; Conrad, E. H.; First, P. N.; de Heer, W. A. *Science* **2006**, *312*, 1191–1196.
- (6) Stankovich, S.; Dikin, D. A.; Piner, R. D.; Kohlhaas, K. A.; Kleinhammes, A.; Jia, Y.; Wu, Y.; Nguyen, S. T.; Ruoff, R. S. *Carbon* **2007**, *45*, 1558–1565.
- (7) Li, D.; Müller, M. B.; Gilje, S.; Kaner, R. B.; Wallace, G. G. *Nat. Nanotechnol.* **2008**, *3*, 101–105.
- (8) Wang, X.; Zhi, L.; Müllen, K. *Nano Lett.* **2008**, *8*, 323–327.
- (9) Dikin, D.; Stankovich, S.; Zimney, E. J.; Piner, R. D.; Dommett, H. B.; Eymenenko, G.; Nguyen, S. T.; Ruoff, R. S. *Nature* **2007**, *448*, 457–460.
- (10) Xu, Y.; Bai, H.; Lu, G.; Li, C.; Shi, G. J. *Am. Chem. Soc.* **2008**, *130*, 5856–5857.
- (11) Blake, P.; Brimicombe, P. D.; Nair, R. R.; Booth, T. J.; Jiang, D.; Schedin, F.; Ponomarenko, L. A.; Morozov, S. V.; Gleeson, H. F.; Hill, E. W.; Geim, A. K.; Novoselov, K. S. *Nano Lett.* **2008**, *8*, 1704–1708.
- (12) Hernandez, Y.; et al. *Nat. Nanotechnol.* **2008**, *3*, 563–568.
- (13) Li, X.; Wang, X.; Zhang, L.; Lee, S.; Dai, H. *Science* **2008**, *319*, 1229–1232.
- (14) Li, X.; Zhang, G.; Bai, X.; Sun, X.; Wang, X.; Wang, E.; Dai, H. *Nat. Nanotechnol.* **2008**, *3*, 538–542.
- (15) Badaire, S.; Poulin, P.; Maugey, M.; Zakri, C. *Langmuir* **2004**, *20*, 10367–70.
- (16) Chakraborty, S.; Chattopadhyay, J.; Guo, W.; Billups, W. E. *Angew. Chem., Int. Ed.* **2007**, *46*, 4486–4488.
- (17) Niyogi, S.; Bekyarova, E.; Itkis, M. E.; McWilliams, J. L.; Hamon, M. A.; Haddon, R. C. *J. Am. Chem. Soc.* **2006**, *128*, 7720–7721.
- (18) McAllister, M. J.; Li, J.-L.; Adamson, D. H.; Schniepp, H. C.; Abdala, A. A.; Liu, J.; Herrera-Alonso, M.; Milius, D. L.; Car, R.; Prud'homme, R. K.; Aksay, I. A. *Chem. Mater.* **2007**, *19*, 4396–4404.
- (19) Pénicaud, A.; Poulin, P.; Derré, A.; Anglaret, E.; Petit, P. *J. Am. Chem. Soc.* **2005**, *127*, 8–9.
- (20) Dresselhaus, M. S.; Dresselhaus, G. *Adv. Phys.* **1981**, *30*, 139–326.
- (21) Vallés, C.; Pénicaud, A. Patent filing FR 07/05803, August 9, 2007.
- (22) Béguin, F.; Setton, R.; Hamwi, A.; Touzain, P. *Mater. Sci. Eng.* **1979**, *40*, 167–173.
- (23) Pénicaud, A.; Valat, L.; Derré, A.; Poulin, P.; Zakri, C.; Roubeau, O.; Maugey, M.; Miaudet, P.; Anglaret, E.; Petit, P.; Loiseau, A.; Enouz, S. *Compos. Sci. Technol.* **2007**, *67*, 795–797.
- (24) Mansour, A.; Razafinimanana, M.; Monthieux, M.; Pacheco, M.; Gleizes, A. *Carbon* **2007**, *45*, 1651–1661.
- (25) Netz, R. R.; Andelman, D. *Encyclopedia of Electrochemistry*; Urbakh, M. M.; Giladi, E., Eds.; Wiley-VCH: Weinheim, Germany, 2002; Vol. 1, pp 282–322.
- (26) Hérold, A. *Physics and Chemistry of Materials with Layered Structures*; Lévy, F., Ed.; Reidel: Dordrecht, The Netherlands, 1979; Vol. 6, p 323.
- (27) Stinchcombe, J.; Pénicaud, A.; Bhayrapa, P.; Boyd, P. W. D.; Reed, C. A. *J. Am. Chem. Soc.* **1993**, *115*, 5212–7.
- (28) Novoselov, K. S.; Jiang, D.; Schedin, F.; Booth, T. J.; Khotkevich, V. V.; Morozov, S. V.; Geim, A. K. *Proc. Natl. Acad. Sci. U.S.A.* **2005**, *102*, 10451–10453.
- (29) Blake, P.; Hill, E. W.; Castro Neto, A. H.; Novoselov, K. S.; Jiang, D.; Yang, R.; Booth, T. J.; Geim, A. K. *Appl. Phys. Lett.* **2007**, *91*, 063124.
- (30) Ferrari, A. C.; Meyer, J. C.; Scardaci, V.; Casiraghi, C.; Lazzeri, M.; Mauri, F.; Piscanec, S.; Jiang, D.; Novoselov, K. S.; Roth, S.; Geim, A. K. *Phys. Rev. Lett.* **2006**, *97*, 187401.
- (31) Casiraghi, C.; Pisana, S.; Novoselov, K. S.; Geim, A. K.; Ferrari, A. C. *Appl. Phys. Lett.* **2007**, *91*, 233108.
- (32) Das, A.; Pisana, S.; Chakraborty, B.; Piscanec, S.; Saha, S. K.; Waghmare, U. V.; Novoselov, K. S.; Krishnamurthy, H. R.; Geim, A. K.; Ferrari, A. C.; Sood, A. K. *Nat. Nanotechnol.* **2008**, *3*, 210.
- (33) Tarascon, J. M.; Di Salvo, F. J.; Chen, C. H.; Carroll, P. J.; Walsh, M.; Rupp, L. J. *Solid State Chem.* **1985**, *58*, 290.
- (34) Petit, P.; Mathis, C.; Journet, C.; Bernier, P. *Chem. Phys. Lett.* **1999**, *305*, 370–374.
- (35) Paolucci, D.; Melle Franco, M.; Iurlo, M.; Marcaccio, M.; Prato, M.; Zerbetto, F.; Pénicaud, A.; Paolucci, F. *J. Am. Chem. Soc.* **2008**, *130*, 7393–7399.

JA808001A